You might find this additional information useful...

This article cites 27 articles, 13 of which you can access free at:
http://jn.physiology.org/cgi/content/full/95/3/1792#BIBL

This article has been cited by 12 other HighWire hosted articles, the first 5 are:

Correlated physiological and perceptual effects of noise in a tactile stimulus
A. Lak, E. Arabzadeh, J. A. Harris and M. E. Diamond
PNAS, April 27, 2010; 107 (17): 7981-7986.
[Abstract] [Full Text] [PDF]

Self-Motion and the Shaping of Sensory Signals
R. A. Jenks, A. Vaziri, A. R. Boloori and G. B. Stanley
J Neurophysiol, April 1, 2010; 103 (4): 2195-2207.
[Abstract] [Full Text] [PDF]

Integration of Vibrotactile Signals for Whisker-Related Perception in Rats Is Governed by Short Time Constants: Comparison of Neurometric and Psychometric Detection Performance
M. C. Stuttgen and C. Schwarz
J. Neurosci., February 10, 2010; 30 (6): 2060-2069.
[Abstract] [Full Text] [PDF]

The Brain in Its Body: Motor Control and Sensing in a Biomechanical Context
H. J. Chiel, L. H. Ting, O. Ekeberg and M. J. Z. Hartmann
J. Neurosci., October 14, 2009; 29 (41): 12807-12814.
[Abstract] [Full Text] [PDF]

Mechanisms of Tactile Information Transmission through Whisker Vibrations
E. Lottem and R. Azouz
J. Neurosci., September 16, 2009; 29 (37): 11686-11697.
[Abstract] [Full Text] [PDF]

Updated information and services including high-resolution figures, can be found at:
http://jn.physiology.org/cgi/content/full/95/3/1792

Additional material and information about *Journal of Neurophysiology* can be found at:
http://www.the-aps.org/publications/jn

This information is current as of May 30, 2010 .

Texture Signals in Whisker Vibrations

Joerg Hipp,[1] Ehsan Arabzadeh,[2] Erik Zorzin,[2] Jorg Conradt,[1] Christoph Kayser,[3] Mathew E. Diamond,[2] and Peter König[1,4]

[1]*University/ETH Zurich, Institute of Neuroinformatics, Zurich, Switzerland.;* [2]*International School for Advanced Studies, Cognitive Neuroscience Sector, Trieste, Italy;* [3]*Max Planck Institute for Biological Cybernetics, Physiology of Cognitive Processes, Tubingen, Germany; and* [4]*University of Osnabruck, Institute of Cognitive Science, Department of Neurobiopsychology, Osnabruck, Germany*

Hipp, Joerg, Ehsan Arabzadeh, Erik Zorzin, Jorg Conradt, Christoph Kayser, Mathew E. Diamond, and Peter König. Texture signals in whisker vibrations. *J Neurophysiol* 95: 1792–1799, 2006. First published December 7, 2005; doi:10.1152/jn.01104.2005. Rodents excel in making texture judgments by sweeping their whiskers across a surface. Here we aimed to identify the signals present in whisker vibrations that give rise to such fine sensory discriminations. First, we used sensors to capture vibration signals in metal whiskers during active whisking of an artificial system and in natural whiskers during whisking of rats in vivo. Then we developed a classification algorithm that successfully matched the vibration frequency spectra of single trials to the texture that induced it. For artificial whiskers, the algorithm correctly identified one texture of eight alternatives on 40% of trials; for in vivo natural whiskers, the algorithm correctly identified one texture of five alternatives on 80% of trials. Finally, we asked which were the key discriminative features of the vibration spectra. Under both artificial and natural conditions, the combination of two features accounted for most of the information: The *modulation power*—the power of the part of the whisker movement representing the modulation due to the texture surface—increased with the coarseness of the texture; the *modulation centroid*—a measure related to the center of gravity within the power spectrum—decreased with the coarseness of the texture. Indeed, restricting the signal to these two parameters led to performance three-fourths as high as the full spectra. Because earlier work showed that modulation power and centroid are directly related to neuronal responses in the whisker pathway, we conclude that the biological system optimally extracts vibration features to permit texture classification.

INTRODUCTION

The whiskers are one of the principal sources of sensory information for rodents; a conspicuous and specialized sensory pathway has evolved to process vibrissal signals. Since the discovery of rodent barrel cortex (Woolsey and Van der Loos 1970), great strides have been made in understanding the relationship between the circuitry and the physiological properties of neurons (Armstrong-James and Fox 1987; Brecht et al. 2003; Staiger et al. 2004). In the last few years, research has begun to turn to another aspect of sensory processing: how does neuronal activity represent the real physical objects with which the animal interacts? Through active movement of their whiskers, rats are able to discriminate the shape of small objects, the aperture size of openings, and the distance and location of objects (Brecht et al. 1997; Hutson and Masterton 1986; Krupa et al. 2001). An additional sensory capacity, the focus of the present work, is the discrimination of the surface features of objects; rats can judge the depth and distance between ridges as well as the coarseness of textures (Carvell and Simons 1990, 1995; Guic-Robles et al. 1989). Indeed, when making a texture discrimination by sweeping their whiskers across a surface, rats demonstrate discriminative capacities that rival or exceed those of humans using their fingertips. Here we aim to identify the signals present in whisker movement that give rise to such fine sensory discriminations.

The nature of the signals present in the whiskers is of interest for several reasons. First, whiskers carry out a signal transformation, acting as the interface between external objects and sensory receptor neurons. Whereas in visual system it is readily apparent that sensory receptors transduce the energy of photons, such a straightforward statement cannot be made for the whisker sensory system. To probe a texture, rodents actively move their whiskers at a frequency of ~5–12 Hz (Carvell and Simons 1990, 1995; Harvey et al. 2001). Signals arising from contact with the object surface are conducted toward the follicle, where the primary sensory neurons are situated. In this process, the mechanical properties of whiskers modify the signals in ways that are only recently beginning to be understood (Fend et al. 2003; Hartmann et al. 2003; Neimark et al. 2003). Second, the features of the signals that reach the whisker follicle can give us indications of what to expect in neuronal processing. If sensory processing mechanisms have evolved to take advantage of the most informative features of the physical signal, then identifying those informative features will lead us to more precise hypotheses about neuronal processing mechanisms.

In this study, we investigate which features of the whisker movements are best suited for the discrimination of textures. We use a hardware model of a whisker system as well as in vivo measurements of rat whiskers. Applying a classification algorithm to the power spectra of whisker movements, we identify vibration features which could be extracted to support optimal performance. This leads to a model of texture discrimination that is, we argue, corroborated by recent electrophysiological experiments (Arabzadeh et al. 2005).

METHODS

Hardware model

RECORDING SETUP. To probe textures, rodents actively move their whiskers across them. We simulated this process using metal whiskers

---

(steel wire, Fig. 1*A;* Small Parts, Miami Lakes, FL) fixed at one end to a sensor head (Fig. 1, *B* and *C*), which was mounted perpendicularly to the rotation axis (Fig. 1, *B* and *C*). With the use of a servo motor (Digital Servo S9251, Futaba, Huntsville, AL), the whisker could be swept back and forth (Fig. 1*B*). The motor was controlled by a microprocessor (Atmega163, Atmel, San Jose, CA) interfaced via a serial port to a PC. The whisking frequency was set to 1 Hz, where one sinusoidal cycle was a complete back-and-forth movement.

The texture of interest was placed in front of and orthogonal to the whisker (Fig. 1*B*). A miniature magnetic field sensor (KMZ51 Philips, Philips-Semiconductors, Eindhoven Netherlands), attached near the base of the whisker, recorded the distortions of the magnetic field induced by the movements of the whisker (Fig. 1, *B* and *C*). The motor position was measured via a potentiometer (variable resistor). Motor position and the deflection of the whisker were digitized (National Instruments DAQCard-6036E, Austin, TX) at a sampling rate of 4,000 Hz.

ARTIFICIAL WHISKERS. The set of artificial whiskers consisted of 4 metal whiskers with the same diameter (0.305 mm) but different length (*W94*: 94 mm; *W88*: 88 mm; *W77*: 77 mm; *W73*: 73 mm). To determine the fundamental resonance frequencies and the damping coefficients as two characteristic features for each whisker, we fixed one end and then deflected and released the free tip, fitting a damped

oscillation to the resulting motion. The resonance frequencies of the whiskers under these conditions ranged from 20 to 40 Hz (*W94*: 23.9 Hz; *W88*: 27.2 Hz; *W77*: 35.3 Hz; *W73*: 40.1 Hz) and the damping coefficient was 1.1 ± 0.15 (SD) s for all whiskers. However, these values do not apply to the more complex boundary condition that occurred while sweeping a whisker across a texture; in that case, the whisker was partly fixed at the "free" end.

TEXTURES. We recorded whisker movements across eight sandpapers of different coarseness. Coarseness is routinely defined by the *P* value, a standard measure of grain size and density (http://www. fepa-abrasives.org/). The eight sandpapers (and average grain diameter) were P40 (425 μm), P60 (269 μm), P80 (201 μm), P100 (162 μm), P120 (125 μm), P150 (100 μm), P180 (82 μm), and P240 (58.5 μm).

PROCESSING OF METAL WHISKER SIGNALS. Whisker movement resulted in a superposition of the deflection signal and the earth magnetic field. To correct for the earth magnetic field, we measured its contribution at each motor position and subtracted it from the total recorded signal. In one whisking cycle, a whisker moved across the surface two times, analogous to the protraction/retraction cycle in natural whisking. Around the inflection points, where the movement direction reversed, the metal whiskers did not contact the texture but
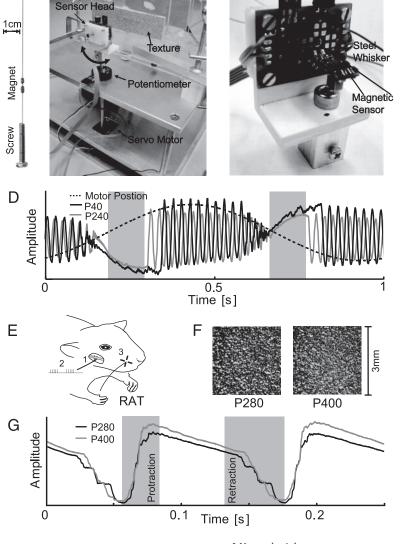

FIG. 1. *A*: metal whisker provided with little magnets. *B*: metal whisker recording setup. *C*: sensor head with magnetic sensor and attached metal whisker. *D*: time course of whisker (*W73*) signal on the finest (P240, black) and the coarsest (P40, gray) sandpaper and the motor position (dotted line). *E*: in vivo recording setup. *F*: 2 textures (sandpapers P280 and P400). *G*: whisker movement signals on 2 sandpapers (P280, gray; P400, black). The shaded areas in *F* and *G* indicate the intervals when the whiskers are sweeping across the texture.

oscillated at their resonance frequency (Fig. 1*D*). Using motor position as a reference, we discarded these segments and selected those when the whisker touched the texture (gray shading, Fig. 1*D*). We refer to these as sweeps. The two directions were treated separately and gave equivalent results; analyses are based on sweeps in one direction only. After low-pass filtering (150 Hz; chebyshev type II filter of 5th order) and subtracting a polynomial of third order, we applied a Hanning window (raised cosine window) and zero padding (adding zeros in the temporal domain to increase the frequency resolution), and then calculated the power spectra.

In vivo recording

RECORDING SETUP. The data were originally collected as described in Arabzadeh et al. (2005). Experiments were conducted in accordance with National Institutes of Health and institutional standards for the care and use of animals in research. Subjects were 10 adult male 250 to 350 g Wistar rats anesthetized with urethan (1.5 g/kg), and data are presented from one case with the most complete stimulus set; the whisker in this dataset was *C3.* "Electrical whisking " (Brown and Waite 1974; Szwed et al. 2003) was generated by stimulating the right facial nerve (Fig. 1*E*) with 1 to 2 V pulses of 100 μs at 200 Hz for 60 ms to produce whisker protraction, followed by a passive 65 ms whisker retraction (also see Fig. 1 in Arabzadeh et al. 2005). The angle traversed at the whisker base, averaged across all trials and all textures, was 25 $\pm$ 6.1° (mean $\pm$ SD). Horizontal and vertical movements at the base were registered by a two-channel optical sensor, each channel consisting of a light-emitting diode (LED) light source and phototransistor. The two voltage signals were digitized (7,634 samples/s). Whisker movement was recorded in contact with five surfaces of different coarseness for 10 min each [compact disk and 4 sandpapers: P1200 (15.3 μm), P400 (35.0 μm), P280 (52.2 μm), P100 (162 μm); Fig. 1F illustrates P280 and P400].

PROCESSING OF IN VIVO WHISKER SIGNALS. We examined the principal direction of whisker movement, corresponding to the horizontal forward- backward axis. Movement in this axis contained all the texture-specific signals (Arabzadeh et al. 2005) and allowed an analysis in one dimension, similar to that of the metal whiskers (Fig. 1*G*). We extracted 300 protraction and retraction segments for each texture (illustrated by gray backgrounds in Fig. 1*G*). After band-pass filtering (cut off frequency 30 Hz, 150 Hz; chebyshev type II filter of 5th order), we applied a Hanning window, zero padding, and then calculated the power spectra.

Classification

The whisker movements in each sweep across a texture were characterized by their power spectrum, a good representation of whisker kinetics (see Fig. 1, Arabzadeh et al. 2005). However, the frequency resolution and the wide frequency band investigated yielded vectors of several hundred dimensions, unsuitable for classification. To estimate the classification performance supported by whisker movements' power spectrum, we reduced the dimensionality of the data using the generalization of Fisher's linear discriminant to multi dimensions (Fisher transform), applied density estimation, maximum likelihood classification and then documented the results as hit-matrices, fraction correct classified and mutual information. The steps are next described in detail.

GENERALIZATION OF FISHER'S LINEAR DISCRIMINANT (FISHER TRANSFORM). The Fisher transform finds a linear projection such that the classes are best separated (Bishop 1995). This is achieved by maximizing the product of the between-class scatter matrix (S_B) and the inverse of the within-class scatter matrix (S_W)

$$S_B = \sum_t n_t (\mu_t - \mu) \cdot (\mu_t - \mu)^T \qquad (1)$$

$$S_W = \sum_t \sum_{s \in t} (x_s^t - \mu_t) \cdot (x_s^t - \mu_t)^T \qquad (2)$$

where t is the texture class index (8 classes for metal whiskers and 5 for the rat whisker); n_t is the number of samples in class t; x_s^t is the sth sweep from texture class t; μ_t is the mean of class t and μ is the mean over all sweeps. In this notation, we use column vectors and ^{T} indicates the transpose. We refer to this transform as *Fisher transform*.

PARAMETRIC DENSITY ESTIMATION. We approximated the probability distribution of feature vectors pertaining to each texture class by a multi-dimensional Gaussian (*n* dimensions). Given a set of feature vectors x_s^t, e.g., the vector components after the Fisher transform, relating to texture t and sweep s, we computed the class specific means μ_t and covariance matrices Σ_t. This yields an estimation of the probability distribution of the feature vectors for each class

$$p_t(x) = \frac{1}{\sqrt{(2\pi)^n \cdot \det(\Sigma_t)}} \cdot e^{-\frac{1}{2}(x - \mu_t)\Sigma_t^{-1}(x - \mu_t)^T} \qquad (3)$$

CLASS ASSIGNMENT. For classification, we randomly select two disjoint subsets: 100 sweeps for the metal whisker data, 150 sweeps for in vivo data. One subset was used to compute the Fisher transform and to estimate the class probability densities (training). The second subset was used to measure performance. Each sample feature vector of the validation set was then assigned to the texture class with the maximum likelihood

$$c(\phi_t^s) = \frac{\arg \max}{t}(p_t(\phi_i^s)) \qquad (4)$$

Classification results were visualized as a *hit-matrix* (*H*), which contained for each sweep from texture class $t = i$ the probability of being assigned to a class c = j

$$H_{i,j} = w(c = j | t = i) \qquad (5)$$

To quantify the classification performance as a single value, we computed the fraction of correctly classified sweeps

$$C(H) = \frac{\sum_i H_{i,i}}{\sum_i \sum_j H_{i,j}} \qquad (6)$$

To compare classification performance of samples from m different textures (chance level: $1/m$) under two different conditions C_1, C_2, we evaluated the relative performance (R) and the relative performance gain ($G = R - 1$)

$$R = \frac{C_2 - 1/m}{C_1 - 1/m} \qquad (7)$$
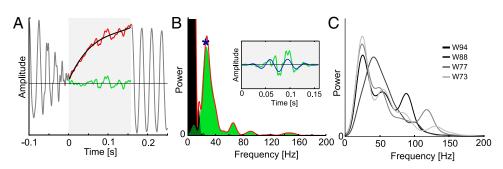
Additionally, we measured the mutual information

$$I(H) = \sum_{i=1}^{m} \sum_{j=1}^{m} w(t = j) \cdot H_{i,j} \cdot \log_2\left(\frac{H_{i,j}}{w(c = j)}\right) \qquad (8)$$

The value of $I(H)$ is in bits.

All data processing was in MATLAB (http://www.mathworks.com).

RESULTS

We first illustrate texture-induced vibrations in the hardware model of the whisker system and introduce a spectral analysis algorithm that yields good classification performance. We then uncover two features of whisker vibration that, by themselves,

FIG. 2. Properties of whisker vibrations. *A*: sweep of the shortest whisker (*W73*) across the coarsest sandpaper (P40). The shaded area indicates the interval when the whisker is sweeping across the texture. The whisker movement (red) is separated into the contribution of bending (black) and modulated part (green). *B*: power spectrum of the trial shown in *A* with whisker movement (red), bending (black), and modulation (green). *C*: average power spectra across all sweeps for all whiskers across the coarsest texture (texture: P40, *W94*: black; *W88*: dark gray; *W77*: gray; *W73*: light gray).

can support a high level of discrimination performance. Finally, we apply this same simple signal processing algorithm to the data obtained in vivo.

Texture-induced vibrations in the hardware model

We analyzed two blocks (*B1, B2*) of 100 sweeps for each of the eight textures (1–8) and four whiskers (*W94, W88, W77, W73*) summing to a total of 6,400 sweeps. An example of two sweeps of the shortest whisker (*W73*) across the coarsest (8, P40) and the finest sandpaper (1, P240) is shown in Fig. 1*D*. The gray shading indicates the period of interest, where the whisker contacted the texture. In Fig. 2, additional stages of signal analysis are shown for whisks on texture 8. The bending of the metal whisker during the sweep becomes evident (Fig. 2*A,* slow shift in red signal); it can be approximated well by a third-order polynomial (Fig. 2*A,* black curve). Because the slow bending parameters were characteristic of a given whisker and its position relative to the texture but not the texture surface, this signal was extracted and was not further analyzed. Once the texture-independent bending was subtracted from the raw signal, the residual signal contained higher frequency components (Fig. 2*A,* green signal). The power spectrum of the raw signal is illustrated in Fig. 2*B* by the red line. The spectrum is also shown broken down into its components: the bending signal (texture-nonspecific) composed of very large power at frequencies up to ~20 Hz (Fig. 2*B,* black area) and the residual signal (Fig. 2*B,* green plot). Thus the separation into bending and residual components corresponded to low- and high-pass filtering, respectively, of the total signal. The peak corresponding to the strongest component in the power spectrum is marked by a blue asterisk. To what extent does the peak of the power spectrum reflect the characteristics of the raw signal? To answer this question, the *inset* of Fig. 2*B* shows the residual signal (green trace, carried over from *A*) overlaid (blue trace) by the 27-Hz predominant frequency component in the signal. This illustrates how the peak value of the power spectrum (asterisk) captured the critical temporal patterns within the raw signal.

Figure 2*C* shows the average power spectra of the residual signal for four different metal whiskers applied to the coarsest texture (8). The shape of the power spectrum was similar, qualitatively, across all whiskers. More than 98% of total power (90% of the residual power) was within the range of 0 to 150 Hz. To summarize, three components of the total signal were excluded: oscillations occurring when the whisker was not in contact with the texture, very low-frequency movements caused by whisker bending, and very high-frequency vibrations (>150 Hz) containing <2% of the total signal power.

Subsequent analysis therefore focuses on the possible texture information carried by the modulation power spectrum at frequencies ≤150 Hz.

Quantifying texture discrimination performance

To quantify the performance we randomly chose distinct subsets of 100 sweeps for training and validation. The parameters for classification were established on the training set. The performance was than evaluated on the validation set (see METHODS). This process was repeated 20 times. Classification is documented by hit-matrices, correct classification percentage, and mutual information.

Overall, classification performance among eight textures using the modulation power spectrum was ~39% correct (chance performance = 12.5%) with a mutual information of 0.83 bits (upper limit = 3 bits). Performance also varied slightly across whiskers (*W94*: 36%; *W88*: 40%; *W77*: 36%; and *W73*: 47%). The SD of the classification across repeated tests was low (maximum: ±3%), indicating the robustness of the classification algorithm. The hit-matrices (Fig. 3*A*) reveal that misclassification mainly resulted from confusing textures of similar coarseness. Averaging of all whiskers (Fig. 3*B*) shows that 47% of all errors arose from confusing neighboring textures (chance: 25%). The total number of neighbors with a certain distance decreases with the distance (e.g., 14 neighbors of distance 1 but just 2 neighbors of distance 7); to account for this, in Fig. 3*C*, we show mean error probability for each distance. Chance corresponds to equally distributed errors (dotted line). This reveals that the classifier extracted coarse-
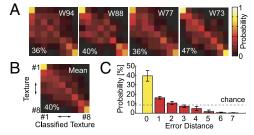

FIG. 3. Classification: metal whiskers. *A*: hit matrices and classification performance for all artificial whiskers. The hit matrices illustrate the probability of assigning a certain texture stimulus (*y* axis) to a specific texture class (*x* axis). The textures are sorted by their coarseness (1, fine, to 8, coarse). Correct classifications fall on the diagonal; confusion of neighboring textures on the coarseness scale (e.g., confusion of 1 and 2) falls on the first off-diagonals, etc. Thus the hit matrices represent correct discriminations as well as the distribution of the classification error. *B*: average of hit matrices in *A*. *C*: distribution of the distance between assigned texture and actual texture on the coarseness scale. The values are corrected for the fact that there are fewer distant than close neighbors. Error bars indicate the SD across whiskers.
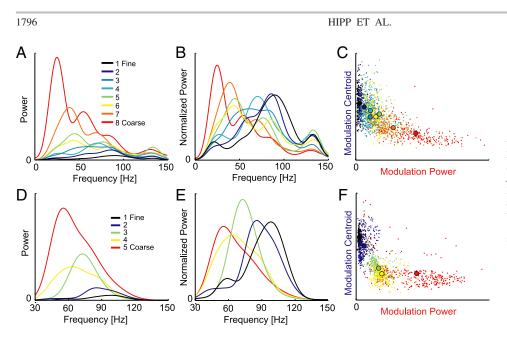
FIG. 4. Meaningful features. Power spectra of movements of the shortest metal whisker (*W73, A–C*) and the real whisker (*D–F*) across different textures is shown color coded, *A* and *D*: Average power spectrum of modulation part shown for all sandpapers individually. *B* and *E*: normalized average power spectrum of the modulation part for all sandpapers. *C* and *F*: modulation power and centroid of all sweeps. See results for details.

ness of the surfaces, capturing the inherent order in this feature. In other words, the power spectrum classifier was measuring the *P* rating of each texture. Discriminating between just the coarsest and finest textures (8 and 1) yielded a performance of 93% and a mutual information of 0.69 bits (upper limit = 1 bit). Thus the information in the modulation power spectrum of one sweep with one whisker was sufficient to support above-chance discrimination between textures of similar coarseness and to reliably discriminate between a coarse and a fine texture.

Spatial and temporal integration of information

Behavioral studies reveal that rats, while probing textures in a discrimination task, contact the surface with many whiskers over several whisking cycles (Carvell and Simons 1990). Thus rats might normally reach optimal performance by combining the signals from different whiskers (*spatial integration*), while collecting data over time (temporal integration). To learn more about how performance could be improved through spatial and temporal integration, we combined the signals acquired from multiple whiskers and multiple sweeps. With a single whisker, the performance using two, three, and four sweeps was 48 ± 6, 55 ± 6, and 59 ± 6%, respectively. This corresponds to a relative performance increase (see METHODS) of 29, 55, and 69% compared with that of a single sweep. Thus increasing the number of whisking cycles is a potentially powerful way to increase the performance.

We also measured the classification performance using several sweeps from distinct whisker/direction combinations. For four whiskers and two directions there exist 28, 56, and 70 possible combinations of two, three, and four sweeps, respectively. The average performance was 50 ± 4, 57 ± 4, and 62 ± 5% corresponding to a relative performance increase of 36, 62, and 80% compared with a single sweep. Similarly to temporal integration, each additional whisker added progressively less performance improvement. However, the average performance increase achieved by spatial integration was greater than that achieved by temporal integration.

Features of the power spectrum that support texture discriminability

In the previous section, we illustrated classification performance based on the complete modulation power spectrum over the range 20–150 Hz. Next, we investigated whether some subset of spectral features was particularly relevant in the classification process. The approach was to look for the texture-specific differences in the power spectra. We compared the power spectra averaged over all sweeps (shortest whisker: *W73,* Fig. 4A). The most evident texture-related difference was the total modulation power in the signal, i.e., the area below the curves. Vibrations induced by coarse textures had high modulation power, while vibrations induced by fine textures had low modulation power. To look for other potentially informative features, we then normalized the area under the curve of all the spectra, thereby excluding modulation power as a feature (Fig. 4B). After this normalization, the peak of the power spectrum emerged as an informative feature: it was at low frequencies for coarse textures and at higher frequencies for fine textures. This could result from the whiskers performing many small jumps while sweeping across a fine texture and fewer, larger jumps across coarse textures. We quantified this feature as the modulation centroid

$$\text{Modulation Centroid} = \int |X(f)|^2 \cdot f^n df \underset{n=2}{=} \int f \cdot |X(f)|^2 df = \int |V(f)|^2 df$$

where $X(f)$ and $V(f)$ are the Fourier transform of the modulation signal and its velocity. For $n = 1$, this corresponds to the center of gravity of the power spectrum. However, we used $n = 2$ as this corresponds to the power in the velocity signal, a quantity which is easy to extract. In Fig. 4C all sweeps of W73 are shown in the space spanned by the modulation power and centroid; color identifies the sandpaper. The signals from the coarsest and the finest sandpapers can be clearly discriminated, while signals from neighboring textures are partially overlapping. Thus a high capacity for texture discrimination appears to be supported by the reduction of the full power spectrum to just two features, power and centroid. This key finding was general to the other metal whiskers.

Next, we quantified the fraction of the classification performance the two features of interest conveyed, relative to the whole spectrum. Performance was tested for each feature singly and for both features together 20 times. The average classification performance using the modulation power alone, modulated centroid alone, and both, were 29 ± 6, 23 ± 3, and 32 ± 6%, respectively. This should be compared with the performance using the whole power spectrum, 39%. The relative performance (*Eq. 7*) is 62, 40, and 74%, respectively. Thus the modulation power and modulation centroid together can account for about three-fourths of the total information available.

Texture signals in rat whisker vibrations

We now turn to the whisker signals recorded during whisking in anesthetized rats (Fig. 1, *E–G*). We used 300 whisks across each of five textures of different coarseness (see Fig. 1*G* for example traces). Similar to the artificial whisker, we extracted the modulation signal by high-pass filtering the whisker movement signal. We separated the protraction and retraction phases of each whisk (Fig. 1*G,* gray shadings) and performed the complete analysis for both phases. Results were qualitatively similar for the two phases, although discrimination performance was slightly lower for the protraction phase. This can be understood by the more structured whisker velocity profile in retraction compared with protraction (see Fig. 1*G* and Fig. 1*B* in Arabzadeh et al. 2005). For these reasons, here we concentrate on the whisker retraction results.

Figure 4*D* shows the average power spectrum of the retraction phase for all five textures. The plotted part of the spectrum (30–150 Hz) covers most of the power (>90%). Just as for the artificial whiskers, the modulation power increased with the coarseness of the texture, whereas the modulation centroid in the normalized power spectrum (Fig. 4E) decreased with the coarseness of the texture. Figure 4*F* shows all sweeps from each texture and the texture means in the space spanned by modulation power and modulation centroid. Except for neighboring textures on the coarseness scale, the sweeps were well separated.

To quantify the reliability afforded by power and centroid, we compared the classification performance based on the whole power spectrum to the classification performance based on just these two features. More precisely, we split the 300 sweeps across each texture randomly into training and validation sets of 150 sweeps each. The classification was performed 20 times, and the mean ± SD of correct performance were derived. Using the whole power spectrum, the performance was 91 ± 1%, whereas using the modulation power and centroid yielded 78 ± 1% correct classified. The modulation power and centroid thus captured, by themselves, 83% of the texture discrimination performance available in the whole power spectrum.

Model of signal processing in the somatosensory system

Motivated by the finding that approximately three-fourths (>80% for real whiskers) of the texture information could be captured by the modulation power and centroid, we propose a model for simple and rapid texture discrimination applicable to both the metal whiskers and the natural whiskers (Fig. 5). First,
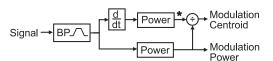

FIG. 5. Evaluation of modulation power and modulation centroid by a combination of band-pass filters (including temporal derivative) and a division operation. *, link to physiological experiments (see DISCUSSION).

the signal is band-pass filtered to extract the relevant modulation signal (in the case of metal whisker: ~20 and 150 Hz cut-off frequencies, real whisker: 30 and 150 Hz cut-off frequencies). Measuring the power in the band-pass filtered signal gives the modulation power. In parallel, the temporal derivative of the band-pass filtered signal is taken, which corresponds to multiplication of the power spectrum by f^2. Determining the power of the velocity signal and normalizing it by the total power in the high pass filtered signal yields the modulation centroid. Thus the main features contributing to texture discrimination, under these experimental conditions, can be extracted by three simple operations: band-pass filtering, temporal differentiation and normalization. In the DISCUSSION, we will explore the possibility that neuronal activity observed in the rat whisker sensory system (Arabzadeh et al. 2005) is a representation of these two whisker vibration features.

DISCUSSION

As a rodent palpates an object, what signals are transmitted from the whisker shaft to the sensory receptor neuron to initiate the process of sensory discrimination? In the present study, the whisker vibration frequency power spectrum obtained from single sweeps permitted our classification algorithm to correctly decode the contacted texture from among textures of varying coarseness on ~80% of trials for real whiskers and 40% for metal whiskers. As shown for the metal whiskers, this performance can be improved by combining the signals from different whiskers (spatial integration) and by collecting data over several sweeps (temporal integration). Because sensory systems may optimize discriminations by transmitting only the most relevant stimulus features to the brain, we asked whether the power spectrum could be reduced to some fundamental features while still allowing reliable classification. The modulation power—the power of the part of the whisker movement representing the modulation due to the texture surface—increased with the coarseness of the texture. The modulation centroid, a measure related to the center of gravity within the power spectrum, decreased with the coarseness of the texture. After condensing the power spectrum to modulation power and modulation centroid, the classification algorithm retained approximately three-fourths of its discriminative performance. Thus as few as two features of whisker movements carried the bulk of the information necessary to discriminate among candidate textures.

We analyzed two different types of whiskers, metal whiskers and rat whiskers, in vivo. Metal whiskers provided a controlled setup to allow highly reproducible recording of whisker movements. In contrast to real whiskers, metal whiskers do not change their properties due to abrasion or ageing and are unaffected by changes in humidity or temperature. Therefore they are more applicable to artificial sensing systems. On the other hand, the in vivo setup aimed at providing realistic

natural signals, simulating the whisker movements in the living animal. However, it should be noted that the whisker movements induced by electrical whisking differ from those in awake behaving animals. For instance, in awake animals, the whisker kinetics might be affected by the muscle force applied to the follicle; moreover, the sensory signals picked up by the whiskers appear to lead to rapid modulation of the motor output (Ahissar and Kleinfeld 2003).

For the metal whisker setup, we used eight relatively similar sandpapers, therefore creating a difficult classification problem. In contrast, for the real whisker setup, we used five different textures with more pronounced differences. A direct quantitative comparison of the performance is therefore not possible. Moreover, in both conditions, we measured the percent of correct discriminations among a large number of textures; in behavioral situations, discriminations are commonly made between just two possible stimuli (e.g., forced choice paradigm). Percent correct would be much higher if discriminations were considered between stimulus pairs (also see the following text).

Regardless of the exact parameters of the stimulus set, the fact that the general findings are true for both a natural whisker in vivo and a metal whisker suggests that a whisker need not possess special mechanical properties to generate texture-specific vibrations. Indeed for whiskers of widely differing properties, the sensory system could discriminate textures by performing band-pass filtering (including temporal derivatives) and division operations.

Emerging picture of texture discrimination

To discriminate textures, rodents use active whisking. Previous studies that analyzed the properties of whisker vibrations used passive stimulation of whiskers (Arabzadeh et al. 2003, 2004, Hartmann et al. 2003; Neimark et al. 2003). Passive stimulation by a piezoelectric wafer or by a rotating drum has the great advantage of characterizing the system in a steady state. However, potentially important properties of active whisking are neglected, such as the continuous change in geometry of the whisker relative to the texture. Furthermore, under more natural whisking conditions, the contact point of the whisker with the surface and the forces at the contact point are likely to change continuously, producing a dynamic modulation of the mechanical properties of the system. Here, the whiskers were moved forth and back across textures in an attempt to mimic the dynamics of natural whisking.

The general picture that emerges from the present experiments is that large quantities of information can be introduced into the sensory system through a single whisker. Consistent with this proposal, behavioral experiments demonstrate that the performance of rats in a difficult texture discrimination task remains intact even when the whiskers are clipped from the normal complement of >30 down to 2 (Carvell and Simons 1995). Our results do not rule out the possibility that rats exploit the gradient of mechanical properties across the whisker array, as proposed in the "resonance frequency hypothesis" (Andermann et al. 2004; Hartmann et al. 2003; Metha and Kleinfeld 2004; Moore 2004; Neimark et al. 2003). However, we did not observe prominent resonance frequencies within the analyzed range that carried most power ($\leq$150 Hz). This might

be due to the difference between active and passive whisking discussed in the preceding text.

Relation to behavioral evidence

How does the observed classification performance compare with other available behavioral evidence? In many texture-discrimination tasks, rats decided where to continue at a Y junction based on texture cues (Carvell and Simons 1990; Guic-Robles et al. 1989). In these experiments, the decision was based on a stimulus set of two textures appearing with equal probability, which corresponds to a maximum available information of 1 bit. The difference of the texture cues ranged from smooth surface versus surface with 30-μm grooves spaced 90 μm (Carvell and Simons 1990) to two sandpapers with grain diameters of 400 versus 2,000 μm (Guic-Robles et al. 1989). The behavioral performance discriminating such stimuli was 85% in both studies. The artificial whisker set up in the present study used eight sandpapers with grain diameters ranging from 59 to 425 μm, whereas the four sandpapers and the compact disc in the in vivo recording ranged from smooth (no structure) to 162-μm grains. For a direct comparison, we consider the discrimination performance for the most extreme stimuli. Using the model based on modulation power and centroid on the movements of one whisker in a single trial to classify the coarsest from the finest sandpaper, we observe an average performance of 89% with the artificial whisker and a performance of 95% with the rat whisker. Thus the behavioral performance of the rats is compatible with the results of the simple model proposed here.

Relation to electrophysiological evidence

Many electrophysiological experiments have been performed to reveal the encoding and transformation of whisker deflections along the whisker pathway from the primary stage, the trigeminal ganglion neurons, to barrel cortex. Trigeminal ganglion neurons reliably encode the kinetics of the whisker movement at a very high temporal resolution (Arabzadeh et al. 2005; Deschenes et al. 2003; Gibson and Welker 1983a,b; Lichtenstein et al. 1990; Shoykhet et al. 2000). More specifically, how does electrophysiological evidence from the whisker system relate to the two features, modulation power and centroid? Neurons in the trigeminal ganglion and the barrel cortex of anesthetized rats, when presented with the stimulus set analyzed here, encoded the "equivalent noise level" (ENL) of the texture-induced vibration in their mean firing rates. The neurons encoded the temporal structure of the vibration—the time difference between the high-velocity events—by a matching response probability profile (Arabzadeh et al. 2005). The ENL is mathematically analogous to the product of modulation power and modulation centroid (Fig. 5, *) and could be extracted by upstream neurons via spike count of barrel cortex populations across the whisker sweep.

In summary, the recent electrophysiological experiments support the view that the modulation power and modulation centroid are reflected in neuronal activity and could be extracted explicitly by neurons upstream of barrel cortex.

REFERENCES

Ahissar E and Kleinfeld D. Closed-loop neuronal computations: focus on vibrissa somatosensation in rat. *Cereb Cortex* 13: 53–62, 2003.

Andermann ML, Ritt J, Neimark MA, and Moore CI. Neural correlates of vibrissa resonance; band-pass and somatotopic representation of high-frequency stimuli. *Neuron* 42: 451–463, 2004.

Arabzadeh E, Panzeri S, and Diamond ME. Whisker vibration information carried by rat barrel cortex neurons. *J Neurosci* 24: 6011–6020, 2004.

Arabzadeh E, Petersen RS, and Diamond ME. Encoding of whisker vibration by rat barrel cortex neurons: implications for texture discrimination. *J Neurosci* 23: 9146–9154, 2003.

Arabzadeh E, Zorzin E, and Diamond ME. Neuronal encoding of texture in the whisker sensory pathway. *PLoS Biol* 3: e17, 2005.

Armstrong-James M and Fox K. Spatiotemporal convergence and divergence in the rat S1 "barrel" cortex. *J Comp Neurol* 263: 265–281, 1987.

Bishop M. *Neural Networks for Pattern Recognition.* Oxford, UK: Oxford Univ. Press, 1995.

Brecht M, Roth A, and Sakmann B. Dynamic receptive fields of reconstructed pyramidal cells in layers 3 and 2 of rat somatosensory barrel cortex. *J Physiol* 553: 243–265, 2003.

Brecht M, Preilowski B, and Merzenich MM. Functional architecture of the mystacial vibrissae. *Behav Brain Res* 84: 81–97, 1997.

Brown AWS and Waite PME. Responses in the rat thalamus to whisker movements produced by motor nerve stimulation. *J Physiol* 238: 387–401, 1974.

Carvell GE and Simons DJ. Biometric analyses of vibrissal tactile discrimination in the rat. *J Neurosci* 10: 2638–2648, 1990.

Carvell GE and Simons DJ. Task- and subject-related differences in sensorimotor behavior during active touch. *Somatosens Mot Res* 12: 1–9, 1995.

Deschenes M, Timofeeva E, and Lavallee P. The relay of high-frequency sensory signals in the whisker-to-barreloid pathway. *J Neurosci* 23: 6778–6787, 2003.

Fend M, Bovet S, Yokoi H, and **Pfeifer R.** An active artificial whisker array for texture discrimination. *Proc IEEE/RSJ Intl Conf Intell Robots Syst* II: 1044–1049, 2003.

Gibson JM and Welker WI. Quantitative studies of stimulus coding in first-order vibrissa afferents of rats. II. Adaptation and coding of stimulus parameters. *Somatosens Res* 1: 95–117, 1983a.

Gibson JM and Welker WI. Quantitative studies of stimulus coding in first-order vibrissa afferents of rats. I. Receptive field properties and threshold distributions. *Somatosens Res* 1: 51–67, 1983b.

Guic-Robles E, Valdivieso C, and Guajardo G. Rats can learn a roughness discrimination using only their vibrissal system. *Behav Brain Res* 31: 285–289, 1989.

Hartmann MJ, Johnson NJ, Towal RB, and Assad C. Mechanical characteristics of rat vibrissae: resonant frequencies and damping in isolated whiskers and in the awake behaving animal. *J Neurosci* 23: 6510–6519, 2003.

Harvey MA, Bermejo R, and Zeigler HP. Discriminative whisking in the head-fixed rat: optoelectronic monitoring during tactile detection and discrimination tasks. *Somatosens Mot Res* 18: 211–222, 2001.

Hutson KA and Masterton RB. The sensory contribution of a single vibrissa's cortical barrel. *J Neurophysiol* 56: 1196–1223, 1986.

Krupa DJ, Matell MS, Brisben AJ, Oliveira LM, and Nicolelis MA. Behavioral properties of the trigeminal somatosensory system in rats performing whisker-dependent tactile discriminations. *J Neurosci* 21: 5752–5763, 2001.

Lichtenstein SH, Carvell GE, and Simons DJ. Responses of rat trigeminal ganglion neurons to movements of vibrissae in different directions. *Somatosens Mot Res* 7: 47–65, 1990.

Metha SB and Kleinfeld D. Frisking the whiskers: patterned sensory input in the rat vibrissa system. *Neuron* 41: 181–184, 2004.

Moore CI. Frequency-dependent processing in the vibrissa sensory system. *J Neurophysiol* 91: 2390–2399, 2004.

Neimark MA, Andermann ML, Hopfield JJ, and Moore Christopher I. Vibrissa resonance as a transduction mechanism for tactile encoding. *J Neurosci* 23: 6499–6509, 2003.

Shoykhet M, Doherty D, and Simons DJ. Coding of deflection velocity and amplitude by whisker primary afferent neurons: implications for higher level processing. *Somatosens Mot Res* 17: 171–180, 2000.

Staiger JF, Flagmeyer I, Schubert D, Zilles K, Kotter R, and Luhmann HJ. Functional diversity of layer IV spiny neurons in rat somatosensory cortex: quantitative morphology of electrophysiologically characterized and biocytin labeled cells. *Cereb Cortex* 14: 690–701, 2004.

Szwed M, Bagdasarian K, and Ahissar E. Encoding of vibrissal active touch. *Neuron* 40: 621–630, 2003.

Woolsey TA and Van der Loos H. The structural organization of layer IV in the somatosensory region (SI) of mouse cerebral cortex. The description of a cortical field composed of discrete cytoarchitectonic units. *Brain Res* 17: 205–242, 1970.